Supporting Information

Mobility of Condensed Counterions in Ion-Exchange Membranes: Application of Screening Length Scaling Relationship in Highly Charged Environments

Yuxuan Huang[†], Hanqing Fan[†], and Ngai Yin Yip[*,†,‡]

[†] Department of Earth and Environmental Engineering, Columbia University, New York, New York 10027-6623, United States

[‡] Columbia Water Center, Columbia University, New York, New York 10027-6623, United States

([*] Email: n.y.yip@columbia.edu)

Number of Pages: 17

Number of Tables: 6

Number of Figures: 7

THEORY

Mobility of Condensed Counterions in Ion-Exchange Membranes. The effective diffusion coefficient, D_{eff}, of condensed counterions in polyelectrolyte solutions under an externally applied electric field was previously evaluated.[1] The main steps of the derivation are presented below. On a rodlike polyelectrolyte with a uniform spacing of b between fixed charges that is under an externally applied electric field, E, the equation of continuity can be written as

$$\frac{1}{b}\frac{\partial \theta}{\partial t} = -\frac{\partial J}{\partial x} \tag{S1}$$

where θ is number of counterions condensed on the polyelectrolyte per fixed charge, t is time, J is number flux of condensed counterions along the polyelectrolyte, and x is coordinate along the charged line. The ion flux is the product of the number of condensed counterions per unit length, $b^{-1}\theta$, and the velocity of the ion, F/ζ:

$$J = \frac{\theta F}{b\zeta} \tag{S2}$$

where F and ζ are the force and friction coefficient, respectively, experienced by the condensed counterions. The force, F, arises from the electrochemical potential gradient of the condensed counterions, $\mu_{ct,\,c}$:

$$F = -\frac{\partial \mu_{ct,\,c}}{\partial x} \tag{S3}$$

$\mu_{ct,\,c}$ can be expressed as

$$\mu_{ct,\,c} = 2k_B T |z_{ct}| \left(1 - |z_{ct}|\theta\right) \xi \ln\left(\kappa b\right) + k_B T \left[\ln\left(\theta/Q\right) + 1\right] - |z_{ct}| eEx \tag{S4}$$

where k_B is the Boltzmann constant, T is absolute temperature, z_{ct} is counterion valence, ξ is the reduced linear charge density of the polymer, κ is the reciprocal of the screening length, and e is the elementary charge. Q is an internal partition function that is assumed to contain the short-range interactions between the condensed counterions and the polyelectrolyte and is independent of θ. The first two terms on the right-side of the equation represent the chemical potential, whereas the third term reflects the electric potential. Substituting eqs S3 and S4 into S2, the ion flux can be expressed as

$$J = \frac{|z_{ct}| e\theta E}{b\zeta} - \frac{k_B T}{b\zeta}\left(1 - 2z_{ct}^2 \xi\theta \ln(\kappa b)\right)\frac{\partial \theta}{\partial x} \tag{S5}$$

Next, substituting eq S5 into S1 yields the equation of motion:

$$\frac{\partial \theta}{\partial t} = -\frac{|z_{ct}| eE}{\zeta}\frac{\partial \theta}{\partial x} + \frac{k_B T}{\zeta}\frac{\partial}{\partial x}\left[\left(1 - 2z_{ct}^2 \xi\theta \ln(\kappa b)\right)\frac{\partial \theta}{\partial x}\right] \tag{S6}$$

To linearize $\partial\theta/\partial t$ to applications of small E, let $\theta = \theta_0 + \Delta\theta$, where $\theta_0 = \left(1 - 1/|z_{ct}|\xi\right)/|z_{ct}|$ is the uniform value of condensed counterions for $E = 0$, and $\Delta\theta$ is, thus, presumably at the order of E. Partial derivatives of θ may then be replaced by the corresponding derivatives of $\Delta\theta$. In eq S6, replacing θ with θ_0 in the send term on the right side and linearizing the equation of motion by dropping the higher-order term that is explicitly dependent on E yield

$$\frac{\partial \Delta\theta}{\partial t} = \frac{k_B T}{\zeta}\left[1 - 2z_{ct}^2 \xi\theta_0 \ln(\kappa b)\right]\frac{\partial^2 \Delta\theta}{\partial x^2} \tag{S7}$$

From Fick's second law of diffusion, the effective diffusion coefficient, D_{eff}, is then

$$D_{eff} = \frac{k_B T}{\zeta}\left[1 - 2z_{ct}^2 \xi\theta_0 \ln(\kappa b)\right] \tag{S8}$$

Further substituting in $\theta_0 = \left(1 - 1/|z_{ct}|\xi\right)/|z_{ct}|$ produces the expression for condensed counterion diffusion coefficient:

$$D_{eff} = \frac{k_B T}{\zeta}\left[1 - 2\left(|z_{ct}|\xi - 1\right)\ln(\kappa b)\right] \tag{S9}$$

The $\left[1 - 2\left(|z_{ct}|\xi - 1\right)\ln(\kappa b)\right]$ term describes the electrostatic effect experienced by condensed counterions, whereas the remainder $k_B T/\zeta$ term accounts for non-electrostatic effects on diffusivity through the friction coefficient, ζ. In the originating study, the free-ion diffusivity of the condensed counterion is $k_B T/\zeta$.[1] However, the study also acknowledged that actual ion diffusivity without the electrostatic effect could be much smaller than the diffusivity in bulk solution due to roughness of the diffusion surface (of viruses),[1] i.e., spatial effects. Within the water-swollen polymer matrices of ion-exchange membranes (IEMs), permeants migrate through

tortuous paths formed by the water phase, as spaces occupied by polymers are inaccessible. To account for the spatial effect of obstructed diffusion, the Mackie-Meares model is employed in the theoretical framework presented in this study:[2,3]

$$D_i^{\mathrm{m}} = D_i^{\mathrm{s}} \left(\frac{f_{\mathrm{w}}}{2 - f_{\mathrm{w}}} \right)^2 \tag{S10}$$

where D_i^{m} and D_i^{s} are ion diffusion coefficients in membrane and bulk solution phases, respectively, and f_{w} is volume fraction of water in the IEM. Replacing the free-ion diffusivity term in eq S9 by eq S10 (i.e., substituting $k_{\mathrm{B}}T/\varsigma$ with $D_i^{\mathrm{s}}\left[f_{\mathrm{w}}/\left(2 - f_{\mathrm{w}}\right)\right]^2$) and converting the ion diffusion coefficient to absolute ion mobility, u, (i.e., using the Einstein relation $D = uk_{\mathrm{B}}T$)[4,5] yield an analytical expression for the condensed counterion mobility in IEMs, $u_{\mathrm{ct,\,c}}^{\mathrm{m}}$ (eq 4 of the main manuscript):

$$u_{\mathrm{ct,\,c}}^{\mathrm{m}} = u_{\mathrm{ct}}^{\mathrm{s}} \left(\frac{f_{\mathrm{w}}}{2 - f_{\mathrm{w}}} \right)^2 \left[1 - 2\left(\left| z_{\mathrm{ct}} \right| \xi - 1 \right) \ln\left(\kappa b \right) \right] \tag{4}$$

where superscripts m and s refer to IEM and bulk solution, respectively, and subscript ct denotes counterion.

The Debye length, λ_{D}, is[6,7]

$$\lambda_{\mathrm{D}} = \left(\frac{N_{\mathrm{A}} e^2 \sum c_i^{\mathrm{m}} z_i^2}{\varepsilon_{\mathrm{r}} \varepsilon_0 k_{\mathrm{B}} T} \right)^{-1/2} \tag{S11}$$

where N_{A} is the Avogadro constant, e is the elementary charge, ε_0 is the permittivity of vacuum, and z_{i} is ion valence. c_i^{m} is the water volume-based molar concentration of counter-/ co-ions in the membrane matrix and is determined using the Donnan-Manning model.[8–10] ε_{r} is the dielectric constant in the membrane matrix, estimated using volume-average dielectric constants of water and dry polymer.[11]

METHOD

Analysis of Model Predictions Against Experimental Observations. The normalized root-mean-square deviation, NRMSD, is a measure of the differences between observed and predicted values and is calculated using[12]

$$\mathrm{NRMSD} = \sqrt{\frac{\sum_{1}^{n}\left(\sigma^{\mathrm{m}}_{\mathrm{Model}} - \sigma^{\mathrm{m}}_{\mathrm{Exp}}\right)^{2} w_i}{\sum_{1}^{n} w_i}} \Bigg/ \frac{\sum_{1}^{n} \sigma^{\mathrm{m}}_{\mathrm{Exp}} w_i}{\sum_{1}^{n} w_i} \tag{S12}$$

where σ^{m} is membrane conductivity, subscripts Model and Exp denote model and experimental values, respectively, and n is total number of samples. Mean of at least triplicate measurements on the same membrane coupon are used for $\sigma^{\mathrm{m}}_{\mathrm{Exp}}$. w is the weighting factor to account for standard deviations of experimental measurements and is define as $w = 1/\left(\delta^{\mathrm{m}}_{\mathrm{Exp}}\right)^{2}$. Alternatively, the difference between observed conductivity and modeled membrane conductivity, $\sigma^{\mathrm{m}}_{\mathrm{Exp}} - \sigma^{\mathrm{m}}_{\mathrm{Model}}$, can be directly expressed as the residual, with standard deviations of the residuals calculated by propagation of uncertainties (results presented in Figure S7).

RESULTS

Illustrative Calculations for Membrane Conductivity Modeling. An illustrative set of sample calculations is presented below for the modeling of CEM conductivity in NaCl solution at 298 K.

For CEM in 1.0 eq/L NaCl solution, the concentrations of counter- and co-ions in the membrane matrix and the fractions of condensed and uncondensed counterions are first calculated using the Donnan-Manning model.[8–10] $\xi = 1.5$, $f_w = 0.285$, SD = 0.279, and IEC = 2.02 meq/g (data are available in Tables S2 and S3). The mean activity coefficients in bulk solution are predicted using the Pitzer model.[13,14]

Membrane counterion concentration, $c_{ct}^{m} = 2.12$ mol/L of swollen membrane

Membrane co-ion concentration, $c_{co}^{m} = 0.0611$ mol/L of swollen membrane

Fraction of condensed counterion, $\phi_c = 0.324$

Fraction of uncondensed counterion, $\phi_u = 0.676$

With absolute mobilities of Na^+ and Cl^- in the bulk solution at 298 K ($u_{ct}^{s} = 3.23 \times 10^{11}$ m^2/sJ and $u_{co}^{s} = 4.93 \times 10^{11}$ m^2/sJ)[15], $z_{ct} = 1$, $z_{co} = -1$, and $\nu_{ct} = \nu_{co} = 1$, eqs 2 and 3 in the main text are used to determine the mobilities of uncondensed counterion and co-ion in the membrane matrix:

Mobility of uncondensed counterion in the membrane, $u_{ct,u}^{m} = 8.24 \times 10^{9}$ m^2/sJ

Mobility of co-ion in the membrane, $u_{co}^{m} = 1.26 \times 10^{10}$ m^2/sJ

Next, the mobility of condensed counterion is computed. Using the membrane ion concentrations, the Debye length is determined by eq S11 to be $\lambda_D = 1.73 \times 10^{-10}$ m. The reciprocal of the screening length is $\kappa = 1.20 \times 10^{7}$ m^{-1} (eq 5 of the main manuscript), using b of 1.36 nm (Table S2). Substituting κ and b into eq 4 of the main manuscript yields:

Mobility of condensed counterion, $u_{ct,c}^{m} = 4.58 \times 10^{10}$ m^2/sJ

Finally, substituting the modeled membrane ion concentrations, membrane ion mobilities, and fraction of condensed and uncondensed counterions into eq 9 of the main manuscript gives the CEM conductivity of 0.679 S/m in 1.0 eq/L NaCl solution at room temperature (Table S4).

Membrane Ionic Conductivities.

Table S1. Membrane ionic conductivities, σ^m, from experimental characterizations and model calculations using the original Donnan-Manning transport framework with $u^m_{ct,c} = 0$ for the cation and anion exchange membranes (CEM and AEM, respectively) in various 1.0 eq/L electrolytes. Experimental values are means and standard deviations of at least triplicates on the same membrane coupon.

CEM conductivity (S/m)			AEM conductivity (S/m)		
Electrolyte	Experimental	Model	Electrolyte	Experimental	Model
NaCl	0.461±0.086	0.216	NaCl	0.362±0.027	0.0760
NaBr	0.430±0.052	0.218	KCl	0.362±0.055	0.0760
Na_2SO_4	0.508±0.027	0.193	$MgCl_2$	0.383±0.037	0.0736
KCl	0.958±0.128	0.307	NaBr	0.206±0.022	0.0755
NH_4Cl	1.01±0.12	0.310	$NaNO_3$	0.287±0.008	0.0704
$MgCl_2$	0.111±0.009	0.135	Na_2CO_3	0.376±0.001	0.0369
$MgSO_4$	0.112±0.003	0.102	Na_2SO_4	0.216±0.017	0.0406
$CaCl_2$	0.164±0.004	0.146	$MgSO_4$	0.216±0.008	0.0386
			Na_3PO_4	0.212±0.053	0.0312

IEM Properties.

Table S2. Ion-exchange capacity (IEC), polymer density (ρ_p), Manning parameter (ξ), and mean intercharge distance, b, of the CEM and AEM. IEC and ρ_p values are means and standard deviations of triplicate measurements on different coupons on the same membrane sheet.

	IEC (meq/g)	Polymer density, ρ_p (g/mL)[16]	Manning parameter, ξ (-)[17]	Mean intercharge distance, b (nm)*
CEM	2.02±0.02	1.43±0.01	1.5±0.1	1.36
AEM	1.85±0.04	1.22±0.01	1.6±0.3	1.93

* Estimated based on Manning parameter, ξ, and dielectric constant of the membrane.[11]

Table S3. Swelling degree, SD, and water volume fraction, f_w, of the CEM and AEM in 1.0 eq/L electrolyte solutions or deionized (DI) water. Values are means and standard deviations of triplicate measurements on different coupons on the same membrane sheet.

CEM			AEM		
Electrolyte	SD (g/g)	f_w (-)	Electrolyte	SD (g/g)	f_w (-)
NaCl	0.279±0.003	0.285±0.002	NaCl	0.171±0.005	0.173±0.004
NaBr	0.291±0.012	0.294±0.009	KCl	0.180±0.004	0.180±0.003
Na_2SO_4	0.296±0.008	0.297±0.006	$MgCl_2$	0.175±0.005	0.176±0.004
KCl	0.303±0.008	0.302±0.006	NaBr	0.129±0.012	0.136±0.011
NH_4Cl	0.295±0.018	0.297±0.013	$NaNO_3$	0.151±0.012	0.156±0.010
$MgCl_2$	0.250±0.004	0.263±0.003	Na_2CO_3	0.277±0.006	0.253±0.004
$MgSO_4$	0.257±0.001	0.269±0.001	Na_2SO_4	0.184±0.004	0.183±0.003
$CaCl_2$	0.251±0.001	0.264±0.001	$MgSO_4$	0.211±0.007	0.205±0.005
DI water*	0.299±0.007	0.300±0.005	Na_3PO_4	0.230±0.008	0.219±0.006
			DI water*	0.171±0.003	0.173±0.003

* Na^+ and Cl^- as the counterion in CEM and AEM, respectively.

Condensed Counterions Fractions.

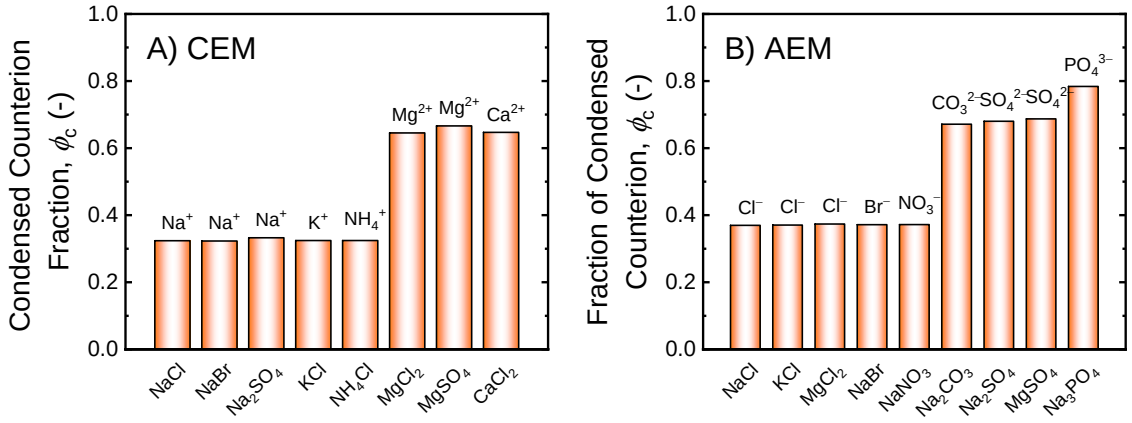

Figure S1. Condensed counterions fractions, ϕ_c, determined using eq 1 of the main manuscript in the A) CEM and B) AEM for different electrolyte solutions. Labels above the columns denote counterions.

Mobilities of Co-ions, Uncondensed Counterions, and Condensed Counterions.

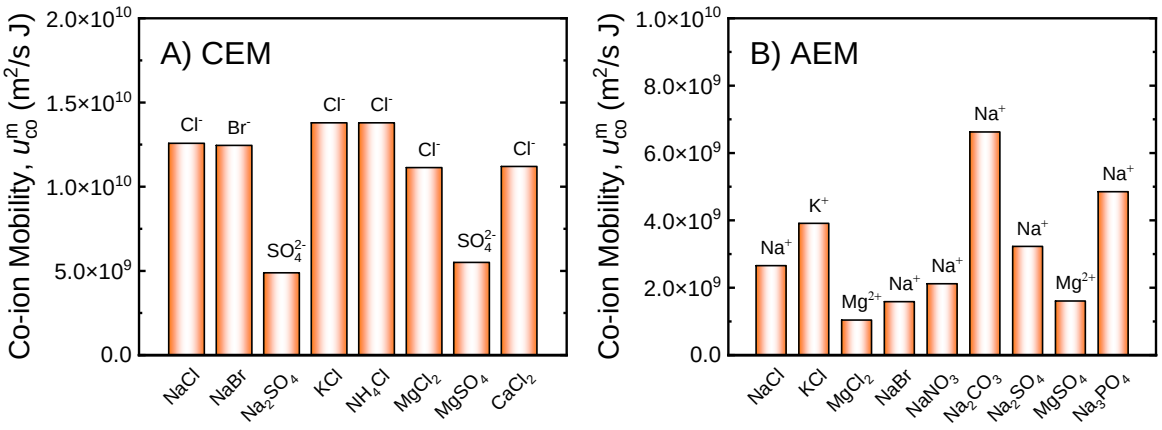

Figure S2. Absolute mobilities of co-ions, u_{co}^{m}, determined using eq 3 of the main manuscript in the A) CEM and B) AEM for different electrolyte solutions. Labels above the columns denote co-ions. Note the different vertical axis scales on the plots.

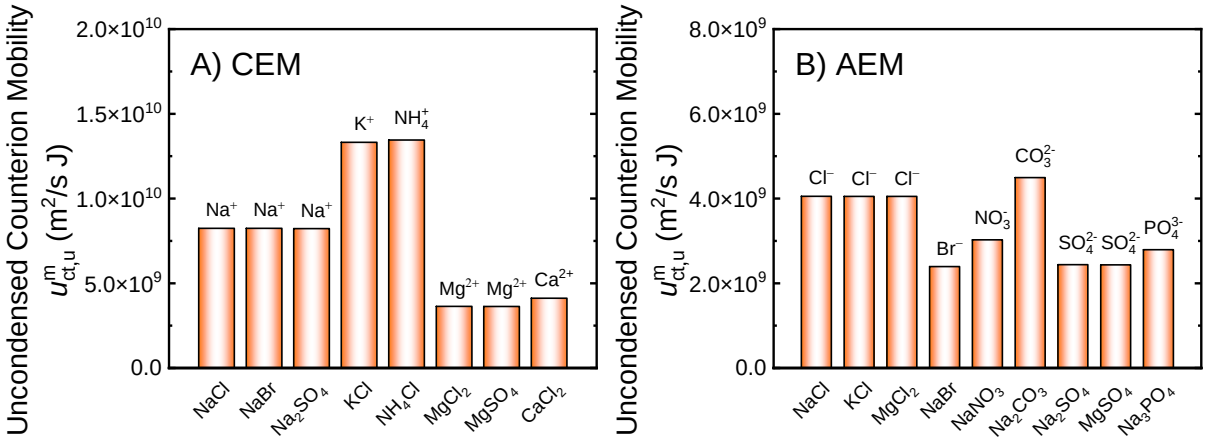

Figure S3. Absolute mobilities of uncondensed counterions, $u_{ct,\,u}^{m}$, determined using eq 2 of the main manuscript in the A) CEM and B) AEM for different electrolyte solutions. Labels above the columns denote counterions. Note the different vertical axis scales on the plots.

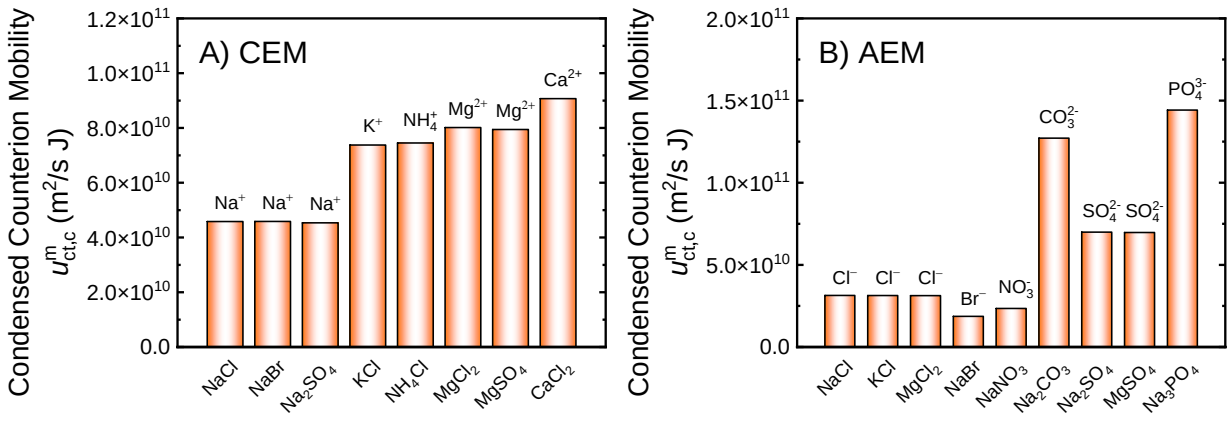

Figure S4. Absolute mobilities of condensed counterions, $u^{m}_{ct,c}$, determined using eq 4 and with screening length computed using eq 6 in the A) CEM and B) AEM for different electrolyte solutions. Labels above the columns denote counterions. Note the different vertical axis scales on the plots.

Membrane Conductivities Incorporating Condensed Counterion Mobility.

Table S4. Membrane ionic conductivities, σ^{m}, from experimental characterizations and model calculations using the Donnan-Manning transport model with $u^{m}_{ct,c}$ determined with eq 4 for the CEM and AEM in various 1.0 eq/L electrolytes. Experimental values are means and standard deviations of at least triplicates on the same membrane coupon. Deviation is defined as $\left(\sigma^{m}_{Model}-\sigma^{m}_{Exp}\right)/\sigma^{m}_{Exp}\times 100\%$.

CEM conductivity, σ^{m} (S/m)				AEM conductivity, σ^{m} (S/m)			
Electrolyte	Experimental	Model	Deviation (%)	Electrolyte	Experimental	Model	Deviation (%)
NaCl	0.461±0.086	0.679	47	NaCl	0.362±0.027	0.415	15
NaBr	0.430±0.052	0.681	58	KCl	0.362±0.055	0.415	15
Na_2SO_4	0.508±0.027	0.656	29	$MgCl_2$	0.383±0.037	0.412	8.0
KCl	0.958±0.128	1.07	12	NaBr	0.206±0.022	0.257	25
NH_4Cl	1.01±0.12	1.08	7.0	$NaNO_3$	0.287±0.008	0.316	10
$MgCl_2$	0.111±0.009	3.60	3.1×10^3	Na_2CO_3	0.376±0.001	4.64	1.1×10^3
$MgSO_4$	0.112±0.003	3.55	3.1×10^3	Na_2SO_4	0.216±0.017	2.78	1.2×10^3
$CaCl_2$	0.164±0.004	4.06	2.4×10^3	$MgSO_4$	0.216±0.008	2.77	1.2×10^3
				Na_3PO_4	0.212±0.053	9.38	4.3×10^3

Contributions of Spatial and Electrostatic Effects to Condensed Counterion Mobility.

Table S5. Magnitude of spatial term, reciprocal of screening length, and magnitude of electrostatic term in determining the condensed counterion mobility (eq 4 of the main manuscript) for various electrolytes in the CEM and AEM.

CEM			
Electrolyte	Spatial term, $\left[f_w/(2-f_w) \right]^2$ (-)	Reciprocal of screening length, κ (m^{-1})	Electrostatic term, $\left[1-2\left(\lvert z_{ct}\rvert \xi -1\right)\ln(\kappa b)\right]$ (-)
NaCl	0.028	1.20×10^7	5.1
NaBr	0.030	1.19×10^7	5.1
Na_2SO_4	0.030	1.26×10^7	5.1
KCl	0.032	1.22×10^7	5.1
NH_4Cl	0.030	1.22×10^7	5.1

AEM			
Electrolyte	Spatial term, $\left[f_w/(2-f_w) \right]^2$ (-)	Reciprocal of screening length, κ (m^{-1})	Electrostatic term, $\left[1-2\left(\lvert z_{ct}\rvert \xi -1\right)\ln(\kappa b)\right]$ (-)
NaCl	0.009	3.16×10^7	7.1
KCl	0.010	3.18×10^7	7.1
$MgCl_2$	0.009	3.22×10^7	7.1
NaBr	0.005	3.06×10^7	7.2
$NaNO_3$	0.007	3.14×10^7	7.1

Influence of Screening Length on Condensed Counterion Mobility. To investigate the overpredictions of condensed multivalent counterion mobilities (as illustrated by Figure 3 of the main manuscript), the role of screening length in the membrane matrix, $1/\kappa$, is analyzed. Condensed counterion mobilities, $u^{m}_{ct,c}$, as functions of the reciprocal of the screening length, κ, are evaluated using eq 4 of the main manuscript and presented as solid curves in Figure S5 for the CEM and AEM in various electrolytes with multivalent counterions (note that both axes are on logarithmic scales). $u^{m}_{ct,c}$ decreases with increasing κ due to weakened electrostatic interactions between membrane fixed charges and condensed counterions.[1] The decline in $u^{m}_{ct,c}$ is especially precipitous as the screening length approaches ≈1 nm, i.e., $\kappa \rightarrow 10^9$ m^{-1}. Dashed horizontal lines

denote condensed counterion mobilities determined from experimentally characterized membrane conductivities (using eq 9 of the main manuscript, with ϕ_c, $u^m_{ct,u}$, and u^m_{co} provided by eqs 1, 2, and 3, respectively).

The intersections of the solid curves and dashed lines, therefore, represent the required κ values for modeled $u^m_{ct,c}$ and σ^m of multivalent counterions to exactly match with experimental observations. However, the intersection κ values are more than two orders of magnitude greater than the screening length reciprocals calculated using the scaling relationship of eq 5 in the main manuscript, indicated by symbols in Figure S5. Such large discrepancies suggest that the screening length scaling relationship expressed by eqs 5 and 6 of the main manuscript may not be appropriate for multivalent ions. The originating studies of the scaling relationship is based on experiments with only monovalent electrolytes, i.e., multivalent ions were not studied,[6,18,19] further substantiating the limited applicability of eqs 5 and 6.

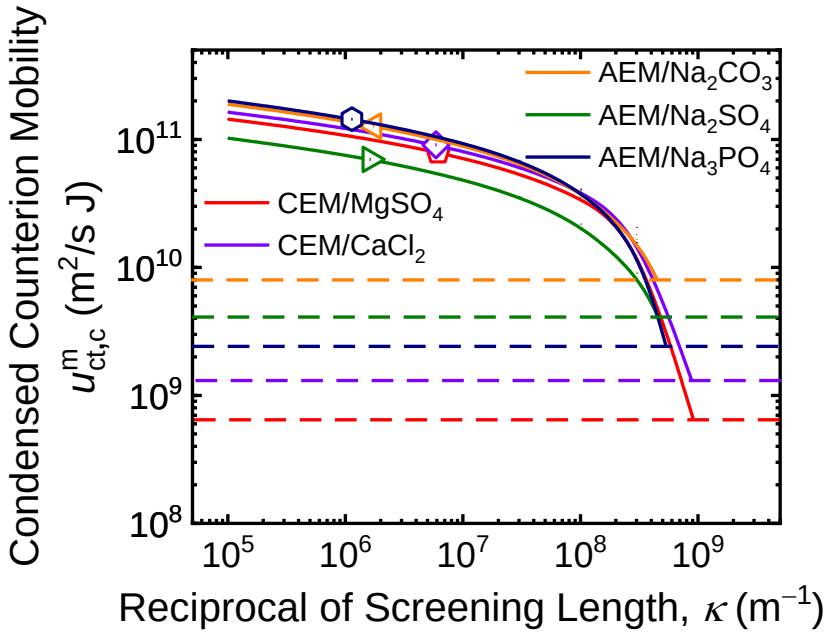

Figure S5. Condensed counterion mobilities, $u^m_{ct,c}$, for multivalent counterions as functions of the screening length reciprocal, κ, evaluated using eq 4 of the main manuscript (solid curves). Dashed horizontal lines represent the condensed counterion mobilities determined from experimentally characterized membrane conductivity using eq 9 of the main manuscript (concentrations of counter- and co-ion in the IEM, c^m_{ct} and c^m_{co},

respectively, are obtained with the Donnan-Manning model, fractions of condensed and uncondensed counterions, ϕ_c and ϕ_u, respectively, are computed using eq 1 and $\phi_u + \phi_c = 1$, and mobilities of co-ion and uncondensed counterion, u_{co}^m and $u_{ct,u}^m$, respectively, are modeled using eqs 3 and 2 of the main manuscript). Symbols signify κ values calculated using eq 5 of the main manuscript.

For multivalent species, we conjecture that the exponent of the power law in the screening length scaling relation, i.e., eq 5 of the main manuscript, is different from the exponent of 3 for monovalent ions. Using eq 4 of the main manuscript and $u_{ct,c}^m$ computed from experimental membrane conductivities (eq 9 of the main manuscript), the required exponents for the power law scaling relation to match modeled values with experimental observations can be back-calculated for the electrolytes with multivalent counterions and are tabulated in Table S6 below. These putative exponents are all very close to the integer value of 1 (within 10%). The power law exponent is, hence, postulated to be unity, and the screening length scaling relation for multivalent ions is, thus, $(\kappa\lambda_D)^{-1} = d/\lambda_D$.

Table S6. Analyzed power law exponents of the screening length scaling relationship for electrolytes with multivalent counterions in the CEM and AEM.

CEM		AEM	
Electrolyte	Exponent	Electrolyte	Exponent
MgCl2	0.91	Na_2CO_3	1.06
MgSO4	0.92	Na_2SO_4	1.05
CaCl2	0.94	$MgSO_4$	1.05
		Na_3PO_4	0.99

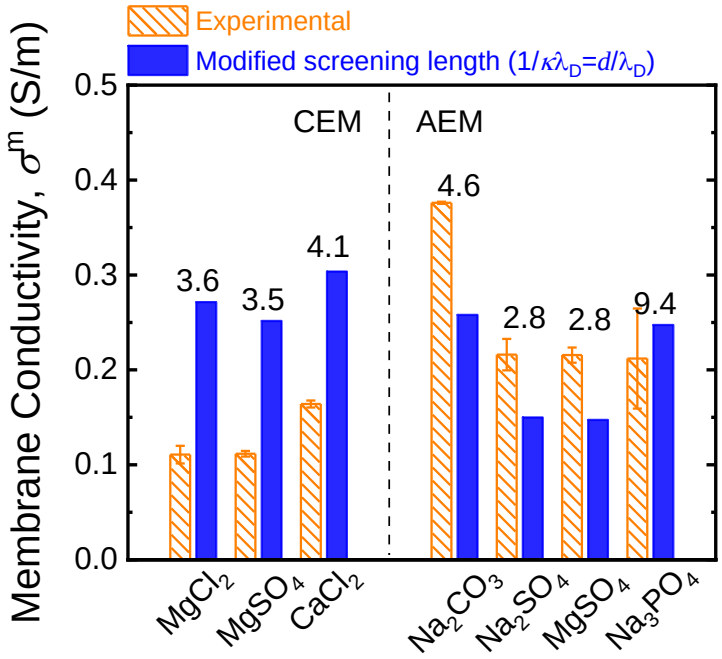

Figure S6. Comparison of membrane conductivities, σ^m, between experimental measurements and modified model predictions (orange hatched and blue filled columns, respectively) for multivalent counterions in the CEM and AEM. The power law exponent of the screening length scaling relationship, eq 5 of the main manuscript, is modified to 1 for the multivalent ions (from the original 3), i.e., $(\kappa\lambda_D)^{-1} = d/\lambda_D$ instead of $(d/\lambda_D)^3$. Labels above the columns indicate modeled σ^m using the original power law exponent of 3 (model results of Figure 3 of the main manuscript).

Residuals of Membrane Conductivity Prediction.

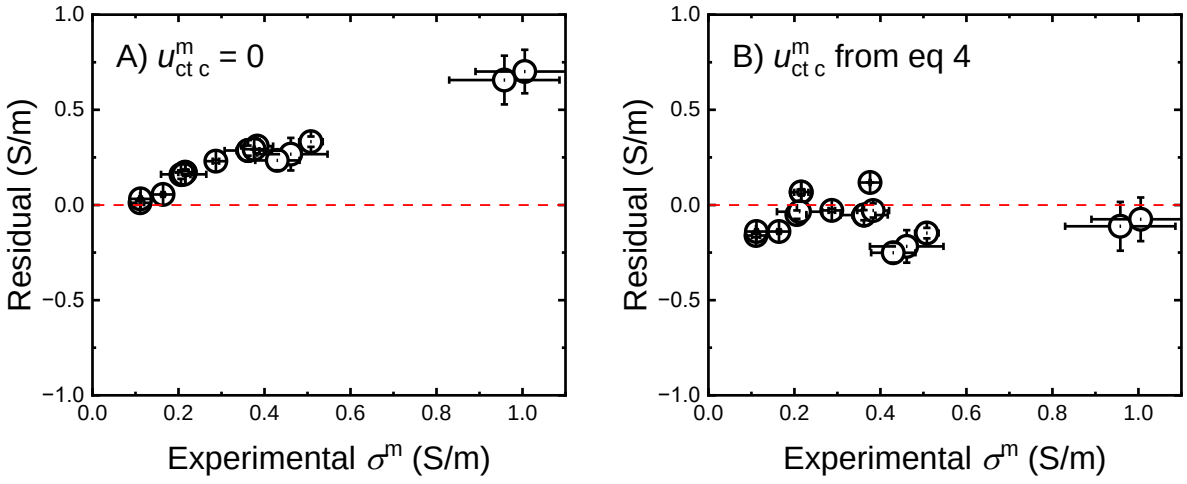

Figure S7. Residuals of membrane conductivities for experimentally characterized σ^{m}. A) Model σ^{m} is determined using the original Donnan-Manning transport model with $u^{m}_{ct,\,c}$ = 0, and B) Model σ^{m} is evaluated using the modifications to the theoretical framework presented here, namely: i) $u^{m}_{ct,\,c}$ is determined by accounting for electrostatic interactions and spatial effects on condensed counterions (eq 4 of the main manuscript), ii) screening length experienced by monovalent counterions is expressed by eqs 5 and 6 of the main manuscript, and iii) screening length for multivalent counterions is described by the modified power law relationship of $(\kappa\lambda_D)^{-1} = (d/\lambda_D)$.

REFERENCES

(1) Manning, G. S. A Counterion Condensation Theory for the Relaxation, Rise, and Frequency Dependence of the Parallel Polarization of Rodlike Polyelectrolytes. *Eur. Phys. J. E* **2011**, *34* (4), 39. https://doi.org/10.1140/epje/i2011-11039-2.

(2) Mackie, J. S.; Meares, P.; Rideal, E. K. The Diffusion of Electrolytes in a Cation-Exchange Resin Membrane I. Theoretical. *Proc. R. Soc. Lond. Ser. Math. Phys. Sci.* **1955**, *232* (1191), 498–509. https://doi.org/10.1098/rspa.1955.0234.

(3) Mackie, J. S.; Meares, P.; Rideal, E. K. The Diffusion of Electrolytes in a Cation-Exchange Resin Membrane. II. Experimental. *Proc. R. Soc. Lond. Ser. Math. Phys. Sci.* **1955**, *232* (1191), 510–518. https://doi.org/10.1098/rspa.1955.0235.

(4) Bard, A. J.; Faulkner, L. R. *Electrochemical Methods: Fundamentals and Applications*, 2nd ed.; Wiley: New York, 2001.

(5) Robinson, R. A.; Stokes, R. H. *Electrolyte Solutions*; Courier Corporation, 2002.

(6) Smith, A. M.; Lee, A. A.; Perkin, S. The Electrostatic Screening Length in Concentrated Electrolytes Increases with Concentration. *J. Phys. Chem. Lett.* **2016**, *7* (12), 2157–2163. https://doi.org/10.1021/acs.jpclett.6b00867.

(7) Gaddam, P.; Ducker, W. Electrostatic Screening Length in Concentrated Salt Solutions. *Langmuir* **2019**, *35* (17), 5719–5727. https://doi.org/10.1021/acs.langmuir.9b00375.

(8) Kitto, D.; Kamcev, J. Manning Condensation in Ion Exchange Membranes: A Review on Ion Partitioning and Diffusion Models. *J. Polym. Sci.* **2022**, 1–45. https://doi.org/10.1002/pol.20210810.

(9) Kamcev, J.; Galizia, M.; Benedetti, F. M.; Jang, E.-S.; Paul, D. R.; Freeman, B. D.; Manning, G. S. Partitioning of Mobile Ions between Ion Exchange Polymers and Aqueous Salt Solutions: Importance of Counter-Ion Condensation. *Phys. Chem. Chem. Phys.* **2016**, *18* (8), 6021–6031. https://doi.org/10.1039/C5CP06747B.

(10) Fan, H.; Yip, N. Y. Elucidating Conductivity-Permselectivity Tradeoffs in Electrodialysis and Reverse Electrodialysis by Structure-Property Analysis of Ion-Exchange Membranes. *J. Membr. Sci.* **2019**, *573*, 668–681. https://doi.org/10.1016/j.memsci.2018.11.045.

(11) Kamcev, J.; Paul, D. R.; Freeman, B. D. Ion Activity Coefficients in Ion Exchange Polymers: Applicability of Manning's Counterion Condensation Theory. *Macromolecules* **2015**, *48* (21), 8011–8024. https://doi.org/10.1021/acs.macromol.5b01654.

(12) Kenney, J. F.; Keeping, E. S. *Mathematics of Statistics*, 3rd ed.; Van Nostrand: New York, 1954.

(13) Pitzer, K. S.; Mayorga, G. Thermodynamics of Electrolytes. II. Activity and Osmotic Coefficients for Strong Electrolytes with One or Both Ions Univalent. *J. Phys. Chem.* **1973**, *77* (19), 2300–2308. https://doi.org/10.1021/j100638a009.

(14) Pitzer, K. S.; Mayorga, G. Thermodynamics of Electrolytes. III. Activity and Osmotic Coefficients for 2–2 Electrolytes. *J. Solut. Chem.* **1974**, *3* (7), 539–546. https://doi.org/10.1007/BF00648138.

(15) Luo, T.; Abdu, S.; Wessling, M. Selectivity of Ion Exchange Membranes: A Review. *J. Membr. Sci.* **2018**, *555*, 429–454. https://doi.org/10.1016/j.memsci.2018.03.051.

(16) Fan, H.; Huang, Y.; Billinge, I. H.; Bannon, S. M.; Geise, G. M.; Yip, N. Y. Counterion Mobility in Ion-Exchange Membranes: Spatial Effect and Valency-Dependent Electrostatic Interaction. *ACS EST Eng.* **2022**, *2* (7), 1274–1286. https://doi.org/10.1021/acsestengg.1c00457.

(17) Kingsbury, R. S.; Zhu, S.; Flotron, S.; Coronell, O. Microstructure Determines Water and Salt Permeation in Commercial Ion-Exchange Membranes. *ACS Appl. Mater. Interfaces* **2018**, *10* (46), 39745–39756. https://doi.org/10.1021/acsami.8b14494.

(18) Lee, A. A.; Perez-Martinez, C. S.; Smith, A. M.; Perkin, S. Scaling Analysis of the Screening Length in Concentrated Electrolytes. *Phys. Rev. Lett.* **2017**, *119* (2), 026002. https://doi.org/10.1103/PhysRevLett.119.026002.

(19) A. Lee, A.; S. Perez-Martinez, C.; M. Smith, A.; Perkin, S. Underscreening in Concentrated Electrolytes. *Faraday Discuss.* **2017**, *199* (0), 239–259. https://doi.org/10.1039/C6FD00250A.